Available online at www.sciencedirect.com

ScienceDirect

Energy Procedia 77 (2015) 331 – 339

Energy Procedia

5th International Conference on Silicon Photovoltaics, SiliconPV 2015

Organic-silicon solar cells exceeding 20% efficiency

Dimitri Zielke[a], Claudia Niehaves[a], Wilfried Lövenich[b], Andreas Elschner[b], Matthias Hörteis[b] and Jan Schmidt[a,c]

[a]*Institute for Solar Energy Research Hamelin (ISFH), Am Ohrberg 1, 31860 Emmerthal, Germany*
[b]*Heraeus Precious Metals, Electronic Materials Division, Chempark Leverkusen, 51368 Leverkusen, Germany*
[c]*Institute of Solid-State Physics, Leibniz Universität Hannover, Appelstr. 2, 30167 Hannover, Germany*

Abstract

After a brief review of the recent evolvement of organic-silicon heterojunction solar cells, we present here our latest measurements of the saturation current densities (J_0) and contact resistances (R_C) of crystalline silicon (c-Si)/poly(3,4-ethylenedioxythiophene):poly(styrenesulfonate) (PEDOT:PSS) junctions. We determine the J_0 values by means of contactless carrier lifetime measurements and the R_C values by comparing sheet resistance measurements with numerical device simulations of the corresponding test structure. Application of an adopted PEDOT:PSS blend and an optimized silicon surface treatment results in a minimal J_0 value of 46 fA/cm², limiting the solar cell open-circuit voltage to V_{oc_limit}=708 mV, and a minimal R_C value of 100 mΩcm². Our optimized silicon surface pre-treatment in combination with the adapted PEDOT:PSS blend are successfully implemented into a cell process with the PEDOT:PSS layer located at the rear surface (the so-called 'BackPEDOT concept'). Record-high efficiencies of 18.3% and of 20.6% are achieved on *n*-type silicon and on *p*-type silicon wafers, respectively. Finally, we compare the internal quantum efficiency of our champion BackPEDOT solar cell with that of a state-of-the-art Al_2O_3/SiN_x-passivated PERC solar cell.

Peer review by the scientific conference committee of SiliconPV 2015 under responsibility of PSE AG

Keywords: Organic-silicon; solar cell; PEDOT:PSS; surface passivation

Peer review by the scientific conference committee of SiliconPV 2015 under responsibility of PSE AG
doi:10.1016/j.egypro.2015.07.047

1. Introduction

The interest in combining organic and inorganic materials for photovoltaic applications has skyrocketed in recent years. Tremendous attention was paid to perovskite materials, where methylammonium is incorporated into an inorganic matrix of lead and iodide. Within few years an impressive efficiency of 20.1% [1] was achieved. However, those remarkable results were obtained on extremely small areas of 0.1 cm^2. An alternative very attractive organic-inorganic approach is the combination of a hole-conducting polymer (such as poly(3,4-ethylenedioxythiophene) : poly(styrenesulfonate) [PEDOT:PSS]) with crystalline silicon to form a new type of heterojunction [2-5]. This organic-silicon heterojunction has already shown to lead to astonishingly low saturation current densities J_0 of 80 fA/cm^2 [6]. PEDOT:PSS on the rear surface of a silicon wafer serves as an emitter for *n*-type silicon and as a 'back-surface-field' for *p*-type silicon. The solar cells made by this so-called 'BackPEDOT concept' [7] were so far strongly limited by a relatively high series resistance (>2 Ωcm²), leading to low fill factors $FF < 70\%$, while open-circuit voltages $V_{oc} > 660$ mV were obtained. Since the commercially available PEDOT:PSS dispersion (Heraeus Clevios™ F HC Solar) was not optimized so far for the application to an organic-silicon heterojunction, we have developed a new PEDOT:PSS blend and an optimized silicon surface treatment. We have transferred our adopted PEDOT:PSS material into an organic-silicon solar cell resulting in a record-high efficiency of 20.6% [8]. In this contribution, we give a brief review of the recent evolvement of organic-silicon heterojunction solar cells. We then analyze our adopted PEDOT:PSS/silicon heterojunction in terms of saturation current density and contact resistance. The new PEDOT:PSS dispersion and our optimized silicon surface pre-treatment are then implemented into organic-silicon heterojunction solar cells.

2. Organic-silicon heterojunction solar cell evolvement

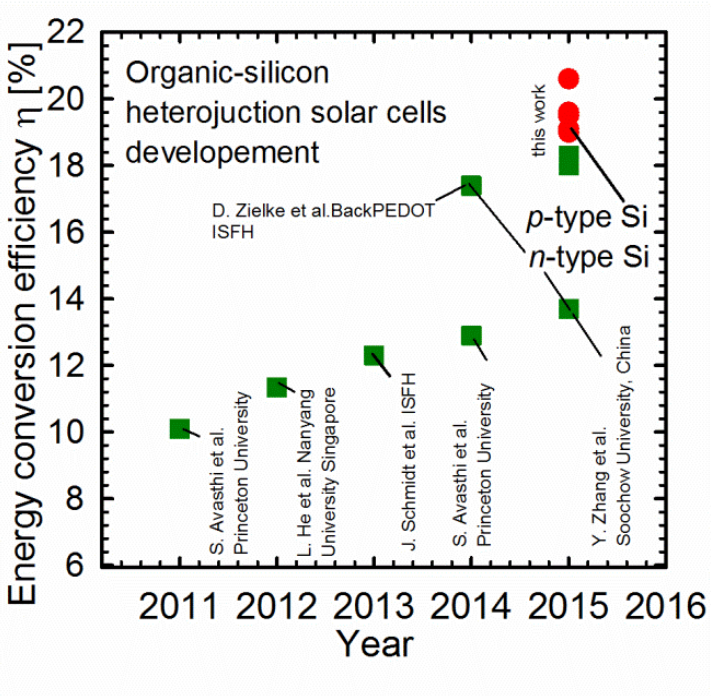

Fig. 1 Organic-silicon heterojunction solar cell efficiency evolvement over time. The organic material used is the hole-conducting PEDOT:PSS for all cells. Solar cells fabricated on *n*-type silicon are shown as green squares, whereas cells made on *p*-type silicon are shown as red circles.

Figure 1 shows reported solar cell efficiencies (η) of PEDOT:PSS/Si solar cells based on silicon wafers over the time period from 2010 to 2015. Details on the published results are given in Table 1. Hybrid solar cells with efficiencies exceeding 10% [2] were realized for the first time in 2011 when PEDOT:PSS was implemented on the top of *n*-type silicon wafers. Further optimization of the PEDOT:PSS blend [5] and/or implementation of an interface layer between silicon and PEDOT:PSS layer [3] resulted in a constant improvement in efficiency over the following years. However, parasitic light absorption of the PEDOT:PSS layer on the front and recombination losses at the insufficiently passivated rear surface limited the efficiency typically to values below 14%. At ISFH, a substantial boost in the efficiency was achieved in 2014 by implementing the PEDOT:PSS layer at the planar rear surface, the so-called 'BackPEDOT concept' [7]. The efficiency of BackPEDOT heterojunction solar cells was very recently further increased from 17.4% [7] to 20.6% [8] by adopting the PEDOT:PSS blend and optimizing the silicon surface pre-treatment.

Table 1. Hybrid organic-silicon solar cell parameters development over the time

Author	Innovation	Year	V_{oc} [mV]	J_{sc} [mA/cm²]	*FF* [%]	η [%]
Avasthi et al.	Silicon wafer as base material [2]	2011	590	29.0	59.0	10.1
He et al.	Native SiO_x as passivating interface between silicon and PEDOT:PSS [3]	2012	600	26.3	70.9	11.3
Schmidt et al.	Random-pyramid-textured front surface and back-surface-field [6]	2013	603	29.0	70.6	12.3
Avasthi et al.	TiO_2 passivating layer on the rear surface [9]	2014	620	29.0	72.1	12.9
Zielke et al.	BackPEDOT concept with PEDOT:PSS on planar rear [7]	2014	653	39.7	67.2	17.4
Schmidt et al.	BackPEDOT with optimal pre-treated *p*-type silicon surface and adapted PEDOT:PSS material [8]	2015	657	38.9	80.6	20.6

3. Organic-silicon junction characterization

3.1. Saturation current density (J_0) measurements

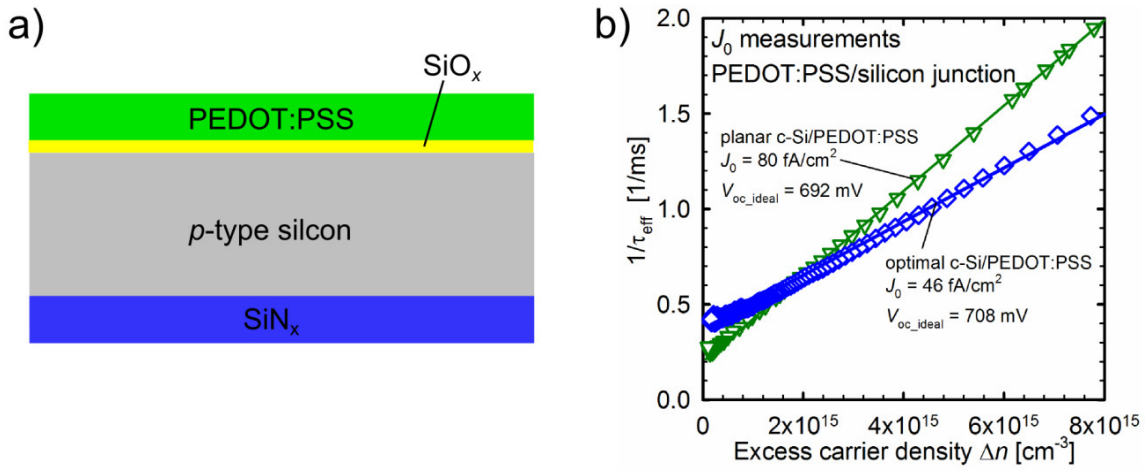

Fig. 2 a) Schematic of a saturation current density test sample and b) saturation current density measurements for a standard PEDOT:PSS (Heraeus Clevios™ F HC Solar) and for our adapted PEDOT:PSS blend.

Figure 2 a) shows a schematic drawing of a saturation current density sample. High resistivity *p*-type float-zone silicon wafers with a doping level N_A=8.9×10^{13} cm^{-3} (ρ=150 Ωcm) and a thickness of 300 µm were used as the base

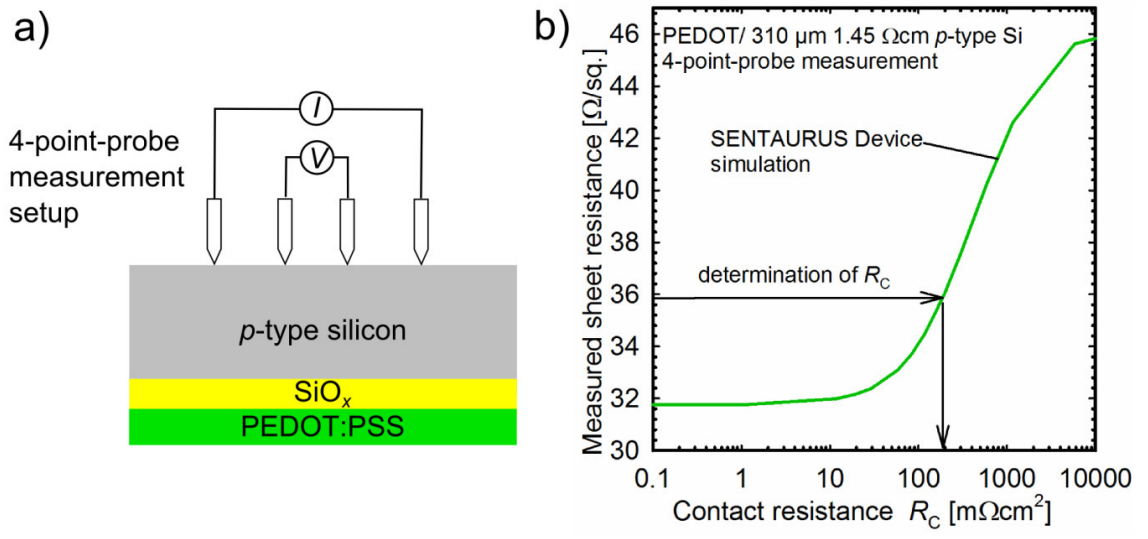

Fig. 3 a) Schematic of a contact resistance sample measured by a 4-point-probe setup and b) simulated sheet resistance R_{sheet} of our 1.45-Ωcm silicon/PEDOT:PSS sample as function of contact resistance R_C.

material for our saturation current density (J_0) test samples. After RCA-cleaning, the rear surface was passivated by a 100 nm thick plasma-enhanced chemical vapour deposited (PECVD) SiN_x layer (refractive index n=2.4 at a wavelength of 632 nm). After rear surface passivation, the silicon front surface was pre-treated or a native SiO_x layer was grown in air. Next, the front surface was spin-coated with PEDOT:PSS dispersion.

The effective carrier lifetime (τ_{eff}) was measured using a Sinton lifetime tester (WCT-120, Sinton Instruments). By plotting the Auger-corrected inverse τ_{eff} as a function of the excess carrier density Δn, the J_0 value was determined applying the method proposed by Kane and Swanson [10].

3.2. Contact resistance (R_C) measurements

In order to extract R_C, we apply here the method introduced by Römer et al. [11]. Figure 3 a) shows a schematic of a contact resistance (R_C) sample measured using a 4-point-probe setup. We use *p*-type silicon with a resistivity of 1.45 Ωcm and a thickness of 310 µm as the base material for our R_C test samples. In order to determine the sheet resistance R_{sheet} of our PEDOT:PSS layer, we use *p*-type silicon with a resistivity of 150 Ωcm and a thickness of 300 µm. After an RCA-cleaning and the silicon surface preparation, various PEDOT:PSS compositions were deposited on the rear surface using a spin-coater.

We measure the sheet resistance (R_{sheet}) of our 150-Ωcm silicon/PEDOT:PSS sample using a Sinton lifetime tester (WCT-120, Sinton instruments). The measured R_{sheet} equals the sheet resistance of the PEODT:PSS layer R_{sheet_PEDOT}, since the conductance of the PEDOT:PSS layer is two orders of magnitude larger compared to the 150-Ωcm silicon wafer. R_{sheet_PEDOT} is used as an input parameter in our device simulations. Another input parameter is the sheet resistance of the silicon wafer $R_{sheet\_Si} = 1.45\ \Omega cm/W$, where W=310 µm is the silicon wafer thickness. Furthermore, we measure R_{sheet} of our 1.45-Ωcm silicon/PEDOT:PSS sample using a 4-point-probe setup (RT-70/RG-7, Napson Corporation), as schematically shown in Fig. 3 a). The 4-point-probe R_{sheet} measurement setup is simulated with SENTAURUS Device [11]. To determine R_C, an artificial layer with an R_{sheet_art} is assumed between silicon and PEDOT:PSS in our simulation. The R_{sheet} value is simulated as a function of R_{sheet_art}. The contact resistance is then calculated using the equation $R_C=R_{sheet\_art}\times A$, where A is the simulated area. Figure 3 b) shows the simulated R_{sheet} of our 1.45-Ωcm silicon/PEDOT:PSS sample as a function of R_C. By comparing the measured R_{sheet} with our simulated R_{sheet} we deduce the R_C value as shown in Fig. 3 b). The two limiting cases are: (i) $R_C \rightarrow \infty \rightarrow R_{sheet} \approx R_{sheet\_Si}$=46.8 Ω/sq and (ii) $R_C \rightarrow 0 \rightarrow R_{sheet} \approx 1/(1/R_{sheet_Si}+1/R_{sheet_PEDOT}) \approx$32 Ω/sq for R_{sheet_PEDOT}=100 Ω/sq.

3.3. Experimental results

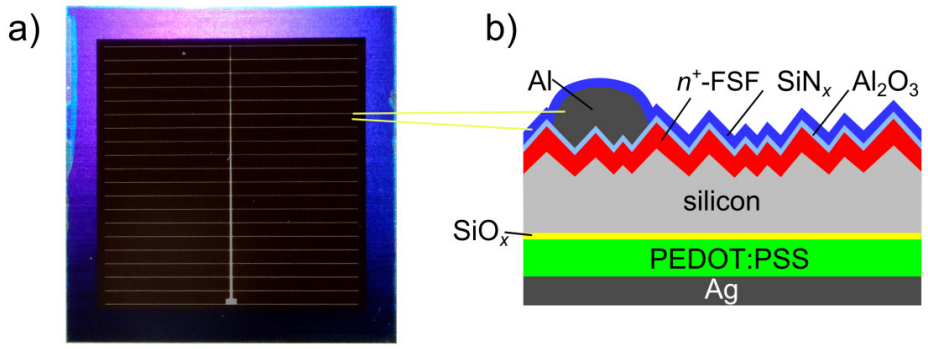

Fig. 4 a) Photograph of our BackPEDOT solar cell front and b) schematic cross-section of the BackPEDOT solar cell.

Figure 3 b) shows J_0 measurements for a standard PEDOT:PSS (Heraeus Clevios™ F HC Solar) and for our adapted PEDOT:PSS blend. The surface pre-treatment of the silicon and our adopted PEDOT:PSS mixture result in a minimum J_0 value of 46 fA/cm^2, which corresponds to a V_{oc_ideal} of 708 mV assuming a J_{sc} of 40 mA/cm². By adapting the PEDOT:PSS blend, an improvement in the maximum limiting V_{oc} of 14 mV was achieved. Importantly, a minimal R_C value of ~100 mΩcm^2 was measured for our optimized organic-silicon heterojunction.

4. Organic-silicon heterojunction solar cells

4.1. Solar cell structure and experimental details

Figure 4 a) shows a photograph of a BackPEDOT solar cell front and b) a schematic cross-section of the BackPEDOT cell. In our process, we start with *n*-type Czochralski-grown (Cz) phosphorus-doped silicon wafers with a resistivity ρ of 1.5 and 5 Ωcm, respectively, and thicknesses of 300 and 160 µm, respectively, as well as *p*-type Float-zone (FZ) boron-doped silicon wafers with a resistivity of 0.5 and 1.5 Ωcm, respectively, and a thickness of 300 µm. All silicon wafers have a (100) surface orientation. The wafers are first laser-cut into 2.49×2.49 cm² large samples. After RCA-cleaning, the samples are protected on both surfaces with a 100 nm thick plasma-enhanced chemical vapor deposited (PECVD) SiN_x layer. On the front surface, a 2×2 cm^2 diffusion window is opened by laser ablation (frequency-doubled Nd:YVO4 laser, SuperRapid, Lumera Laser). Afterwards, the samples are cleaned in a H_2O:HCl:H_2O_2 and H_2O:NH_4OH:H_2O_2 solution at a temperature of 80°C. Within the ablated window the silicon surface is random-pyramid (RP) textured in a KOH/iso-propanol solution. RP-texturing results in ~5 µm large random pyramids on the silicon surface within the ablated window, while the SiN_x-protected area is not affected. Subsequently, after RCA-cleaning, a phosphorus diffusion is performed from a $POCl_3$ source in a quartz-tube furnace at 850°C forming a n^+-layer at the front with a sheet resistance of ~100 Ω/sq and a profile depth of ~0.4 µm. The SiN_x protecting layer and the phosphorus silicate glass are then removed in a 5% hydrofluoric acid solution. After additional RCA-cleaning, an 0.24 nm AlO_x tunneling layer is deposited by means of plasma-assisted atomic layer deposition (FlexAL, Oxford Instruments) on the front surface. A sub-set of samples is processed as passivated emitter and rear cell (PERC) reference solar cells, where the rear surface is passivated by an Al_2O_3/SiN_x stack and locally opened by laser ablation. Next, an aluminum grid is deposited on the cell front through a nickel shadow mask by electron beam evaporation. After metallization, the front surface is coated by a 10 nm surface-passivating SiN_x layer with a refractive index of 2.4 and on top of that by a 70 nm SiN_x antireflection coating with a refractive index of 1.9. Both SiN_x layers are deposited at a temperature of 330°C using PECVD. Afterwards, the samples are annealed in air for 2 min at 350 °C in order to improve the front surface passivation.

Before PEDOT:PSS deposition the samples are dipped in a 1% HF solution for 1 min. After surface preparation or after native SiO_x layer formation, a PEDOT:PSS layer is deposited by spin-coating on the entire rear at 500 revolutions per minute (rpm) for 10 seconds and subsequently 1000 rpm for 30 seconds. The sample was then dried on a hotplate in air at 130 °C for 15 min to remove residual solvents. The resulting PEDOT:PSS thickness is in the range between 50 and 200 nm. Finally, the entire rear surface is metalized with silver (BackPEDOT) or aluminum (PERC reference solar cell) by means of e-gun evaporation (Balzers, BAK).

4.2. Solar cell parameters

Table 2. Measured BackPEDOT and PERC solar cell parameters. The aperture cell area is 4 cm². All measurement were performed at an illumination intensity of 100 mW/cm² and a cell temperature of 25°C.

Base silicon	Cell type	Surface treatment	PEDOT :PSS	V_{oc} mV	J_{sc} mA/cm²	*FF* %	p*FF* %	η %	R_{s_dlt} Ωcm²
0.5 Ωcm *p*-type FZ-Si	PERC	--	--	662	39.7	79.8	82.8	20.9	0.6
0.5 Ωcm *p*-type FZ-Si	BackPEDOT	optimal	adopted	659	36.6	78.8	83.3	19.0	0.9
0.5 Ωcm *p*-type FZ-Si	BackPEDOT	optimal	adopted	653	36.7	79.9	82.7	19.1	0.5
0.5 Ωcm *p*-type FZ-Si	BackPEDOT	optimal	adopted	655	37.1	80.1	83.3	19.5	0.7
1.5 Ωcm *p*-type FZ-Si	BackPEDOT	optimal	adopted	656	37.4	80.1	83.5	19.6	0.6
1.5 Ωcm *p*-type FZ-Si	BackPEDOT	optimal	adopted	657	38.9	80.6	83.2	**20.6**	0.5
1.5 Ωcm *p*-type FZ-Si	BackPEDOT	native SiO_x	adopted	656	38.8	73.9	83.2	18.8	2.1
1.5 Ωcm *p*-type FZ-Si	BackPEDOT	native SiO_x	adopted	657	38.7	73.1	83.2	18.6	2.2
1.5 Ωcm *n*-type Cz-Si	BackPEDOT	native SiO_x	standard	653	39.7	67.2	82.0	17.4	2.9
1.5 Ωcm *n*-type Cz-Si	BackPEDOT	native SiO_x	standard	663	39.0	66.3	81.3	17.1	3.6
5.0 Ωcm *n*-type Cz-Si	BackPEDOT	optimal	adopted	654	36.7	75.1	78.7	18.0	0.8
5.0 Ωcm *n*-type Cz-Si	BackPEDOT	optimal	adopted	654	36.6	76.4	79.8	**18.3**	0.7

Table 2 summarizes the parameters of our BackPEDOT solar cells and a PERC reference solar cell. The measurements were performed at an illumination intensity of 100 mW/cm² at a temperature of 25 °C using a commercial cell-tester (LOANA, PV-tools).

Figure 5 a) summarized the measured open-circuit voltages V_{oc} of our fabricated solar cells. V_{oc} values in the range between 653 and 663 mV are achieved with our BackPEDOT solar cells, which are quite comparable to the V_{oc} of 662 mV of the PERC reference. The similar V_{oc} values of our state-of-the-art AlO_x/SiN_x rear-surface-passivated PERC solar cell and the BackPEDOT cells highlight the excellent passivation quality of our organic-silicon junction. Furthermore, no relevant differences are observable between *n*-type and *p*-type silicon wafers as well as between solar cells on silicon wafers of different doping concentrations.

Figure 5 b) shows the measured short-circuit current-densities J_{sc} of the fabricated solar cells. The PERC reference cell shows a high J_{sc} value of 39.7 mA/cm², whereas the J_{sc} values of our BackPEDOT cells lie in the range between 36.6 and 39.7 mA/cm². We observe that J_{sc} depends on the type of pre-treatment and on the PEDOT:PSS composition. The highest J_{sc} values of 39.0 and 39.7 mA/cm² are achieved with native SiO_x in combination with standard PEDOT:PSS. For BackPEDOT cells with native SiO_x and adopted PEDOT:PSS we measure slightly reduced J_{sc} values of 38.7 and 38.8 mA/cm². Optimally processed silicon in combination with the adopted PEDOT:PSS results in J_{sc} values between 36.6 and 38.9 mA/cm², with a median value of 37.1 mA/cm² (9 BackPEDOT solar cells). The reason for the 2 mA/cm² reduced J_{sc} values of the optimally treated silicon in combination with the adopted PEDOT:PSS compared to the native SiO_x with standard PEDOT:PSS is a topic of ongoing research. The differences in the adhesion properties between native SiO_x and the optimally pre-treated silicon surface may cause different thicknesses of the final PEDOT:PSS layer, which acts as parasitic light absorber [7].

Figure 5 c) compiles the fill factors (*FF*) (filled symbols) and pseudo fill factors (p*FF*) (open symbols) of our solar cells. We observe a positive *FF* trend as a function of our pre-treatment and the PEDOT:PSS composition. The lowest *FF* values of 66.3 and 67.2% are measured on solar cells with native SiO_x plus standard PEDOT:PSS. The low *FF* is caused by increased series resistance (R_s) values of 2.9 and 3.6 cm², respectively. By optimizing the PEDOT:PSS composition, the *FF* was increased to values of 73.1 and 73.9%. The highest *FF* values between 78.8 and 80.6% were achieved by combining the optimally treated silicon surface with the adapted PEDOT:PSS composition. On *n*-type silicon we observe lower *FF*s of 75.1 and 76.4% for our optimally treated silicon surface in combination with the adapted PEDOT:PSS composition caused by lower p*FF*-values of 78.7 and 79.8%. The most

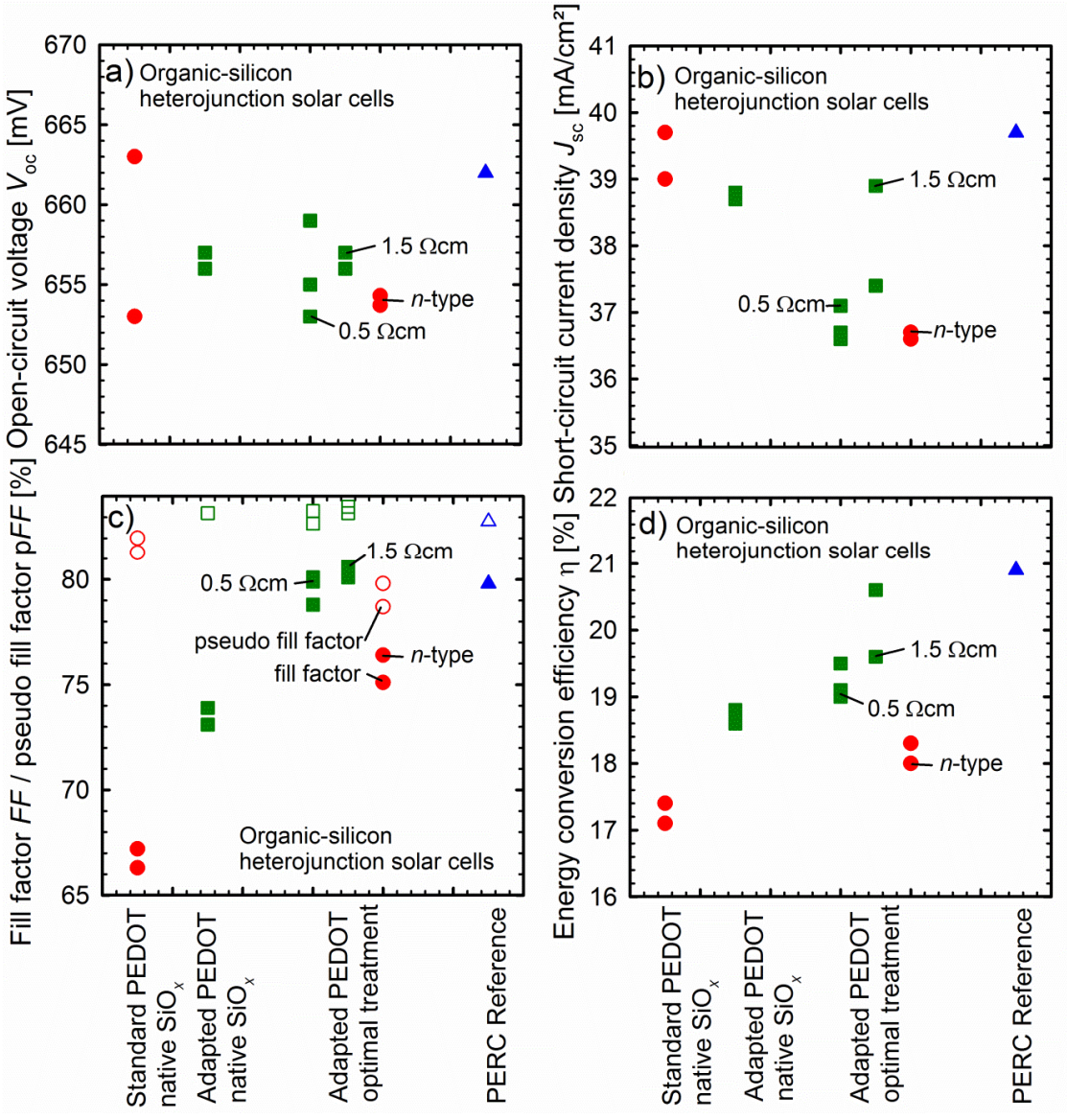

Fig. 5 Measured (a) open-circuit voltages (V_{oc}), (b) short-circuit current densities (J_{sc}), (c) fill factors (filled symbols) (*FF*) and pseudo fill factors (open symbols) (p*FF*) and (d) energy conversion efficiencies (η) of BackPEDOT solar cells on *p*-type (green squares) and *n*-type silicon (red circles) and a PERC reference cell (blue triangles).

likely reason for the reduced p*FF* values are shunts within the silicon/PEDOT:PSS interface. *p*-type BackPEDOT and PERC solar cells show p*FF* values larger than 82.7%. Importantly, all 7 BackPEDOT solar cells with optimally treated *p*-type silicon surface in combination with the adapted PEDOT:PSS combination show R_s-values < 1 Ωcm².

Figure 5 d) shows the measured one-sun energy conversion efficiency η of the fabricated solar cells. The efficiency follows the positive *FF* trend, where the shunted organic-silicon interface limits our *n*-type silicon BackPEDOT solar cells to η values of up to 18.3%. Consequently, for our optimally treated silicon surface plus the adapted PEDOT:PSS composition, we achieve efficiencies in the range between 19.0 and 20.6% on *p*-type silicon wafers.

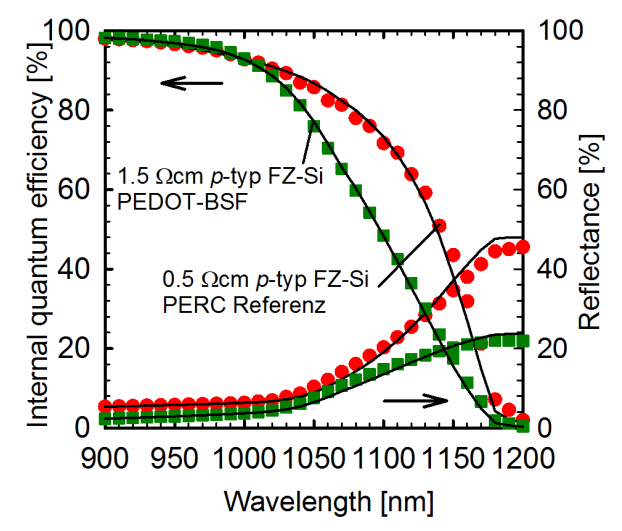

Fig. 6 Measured spectrally resolved internal quantum efficiency *IQE* and reflectance *R* of a *p*-type silicon BackPEDOT cell (green squares) in comparison with a PERC cell.

4.3. Internal quantum efficiency

Figure 6 shows the measured spectrally resolved internal quantum efficiency (*IQE*) and the reflectance measurements of the best BackPEDOT cell (green squares) in comparison with the PERC reference cell (red circles). In the wavelength (λ) range between 900 and 1000 nm our BackPEDOT solar cell shows a very similar performance as the Al_2O_3/SiN_x-passivated PERC solar cell. In this λ range, the *IQE* curve is dominated by the rear surface recombination velocity S_{rear}. Using the parameter-confidence-plot [12], we determined an S_{rear} of (190 ± 60) cm/s and (165 ± 40) cm/s for the PERC and BackPEDOT cells, respectively. Lower *IQE* values for the BackPEDOT solar cell at λ > 1000 nm lead to a reduced J_{sc} value. We attribute the lower *IQE* values of the BackPEDOT cell compared to the PERC reference to the non-optimized PEDOT:PSS layer thickness and hence a pronounced parasitic absorption within the PEDOT:PSS. Reducing the PEDOT:PSS layer thickness is expected to increase the J_{sc}. Also, an adaption of the PEDOT:PSS composition towards a reduced absorption in the infrared wavelengths range might lead to a further improvement in the photocurrent.

4. Conclusions

We briefly reviewed the rapid efficiency improvement of organic-silicon heterojunction solar cells based on the hole-conducting polymer PEDOT:PSS on a crystalline silicon wafer. Within the past 5 years the efficiency increased from 10% to above 20%. Highest efficiencies were achieved with our novel BackPEDOT solar cell architecture,

where the PEDOT:PSS layer is implemented on the planar rear surface of the silicon wafer. By adapting the PEDOT:PSS dispersion and by optimizing the silicon surface pre-treatment we were able to achieve J_0 values of 46 fA/cm² and R_C values of 100 mΩcm². We successfully implemented our optimal silicon treatment and the adapted PEDOT:PSS composition to BackPEDOT solar cells and achieved R_s values < 1 Ωcm² and V_{oc}-values > 653 mV. Our lowest series resistance of 0.5 Ωcm² resulted in a *FF* of 80.6%. Combining the high *FF* value with a short-circuit current density of 38.9 mA/cm², an efficiency of 20.6% was achieved. Further improvements seem to be possible by reducing the parasitic absorption within the PEDOT:PSS within the infrared wavelength range.

References

[1] Noh JH, Im SH, Heo JH, Mandal TH, Seok SI. Efficient, and Stable Inorganic – Organic Hybrid Nanostructured Solar Cells. Nano Letters. 2013; 13: p. 1764-1769.

[2] Avasthi S, Lee S, Loo YL, Sturm JC. Role of Majority and Minority Carrier Barriers Silicon/Organic Hybrid Heterojunction Solar Cells. Adv. Mater. 2011; 23: p. 5762–5766.

[3] He L, Jiang C, Wang H, Lai D, Rusli. High efficiency planar Si/organic heterojunction hybrid solar cells. Appl. Phys. Lett. 2012; 100: p. 073503 1-3.

[4] Pietsch M, Jäckle S, Christiansen S. Interface investigation of planar hybrid n-Si/PEDOT:PSS solar cells with open circuit voltages up to 645 mV and η of 12.6 %. Applied Physics A. 2014; 115: p. 1109-1113.

[5] Zhang Y, Liu R, Lee ST, Sun B. The role of a LiF layer on the performance of poly(3,4-ethylenedioxythiophene):poly(styrenesulfonate)/Si organic-inorganic hybrid solar cells. Appl. Phys. Lett. 2014; 104: p. 083514 1-4.

[6] Schmidt J, Titova V, Zielke D. Organic-silicon heterojunction solar cells: Open-circuit voltage potential and stability. Appl. Phys. Lett. 2013;: p. 183901-1-4.

[7] Zielke D, Pazidis A, Werner F, Schmidt J. Organic-silicon heterojunction solar cells on n-type silicon wafers: The BackPEDOT concept. Sol. Energy Mater. Sol. Cells. 2014; 131: p. 110-116.

[8] Schmidt J, Zielke D. Organic-silicon Heterojunctions: a Promising New Concept for High-efficiency Solar Cells. Proceedings of the 6th WCPEC, Kyoto, Japan. 2014.

[9] Avasthi S, Nagamatsu KA, Jhaveri J, McClain WE, Man G, Kahn A, et al. Double-Heterojunction Crystalline Silicon Solar Cell Fabricated at 250°C with 12.9 % Efficiency. IEEE Journ al of Photovoltaics. 2014;: p. 949-953.

[10] Kane DE, Swanson RM. MEASUREMENT OF THE EMITTER SATURATION CURRENT BY A CONTACTLESS PHOTOCONDUCTIVITY DECAY METHOD. Proc. 18th IEEE PVSC. Las Vegas, USA. 1985;: p. 578-581.

[11] Römer U, Peibst R, Ohrdes T, Lim B, Krügener J, Bugiel E, et al. Recombination behavior and contact resistance of n+ and p+ poly-crystalline Si/mono-crystalline Si junctions. Sol. Energy Mater. Sol. Cells. 2014; 131: p. 85-91.

[12] Brendel R, Hirsch M, Plieninger R, H. WJ. Quantum Efficiency Analysis of Thin-Layer Silicon Solar Cells with Back Surface Fields and Optical Confinement. IEEE Transactions On Electron Devices. 1996; 43: p. 1104-1113.